Pediatr Radiol (2011) 41:1013–1019
DOI 10.1007/s00247-011-2132-1

ORIGINAL ARTICLE

Radiological evaluation of dysmorphic thorax of paternal uniparental disomy 14

Osamu Miyazaki · Gen Nishimura · Masayo Kagami · Tsutomu Ogata

Received: 21 November 2010 / Revised: 31 January 2011 / Accepted: 1 February 2011 / Published online: 24 May 2011

Abstract
Background The "coat-hanger" sign of the ribs with a bell-shaped thorax has been known as a radiological hallmark of the paternal uniparental disomy 14 (upd(14)pat).
Objective To quantitatively determine the differences in thoracic deformity between upd(14)pat and other bone diseases with thoracic hypoplasia and to establish the age-dependent evolution.
Materials and methods The subjects comprised 11 children with upd(14)pat. The angle between the 6th posterior rib and the horizontal axis was measured (coat hanger angle; CHA). The ratio of the mid- to widest thorax diameter (M/W ratio) was calculated for the bell-shaped thorax.
Results CHA ranged from +28.5 to 45° (mean; 35.1°±5.2) in upd(14)pat, and from −19.8 to 21° (−3.3±13°) in bone dysplasias ($p<0.01$). The M/W ratio ranged from 58% to 93% (75.4±10) in upd(14)pat, and from 80% to 92% (86.8±3.3) in bone dysplasias ($p<0.05$). Serial radiographs revealed that CHA remained constant during early childhood, while the M/W ratio gradually increased with age.
Conclusion The "coat-hanger" sign of upd(14)pat provides a distinctive radiological gestalt that makes it possible to differentiate the disorder from other skeletal dysplasias. By contrast, the bell-shaped thorax is significant only in the neonatal period.

Keywords UPD14 · Plain radiograph · Coat-hanger sign · Bell-shaped thorax

O. Miyazaki (✉)
Department of Radiology,
National Center for Child Health and Development,
2-10-1 Okura,
Seatagaya-ku, Tokyo 157-8535, Japan
e-mail: osamu-m@rc4.so-net.ne.jp

G. Nishimura
Department of Radiology,
Tokyo Metropolitan Children's Medical Center,
2-8-29 Musashidai,
Fuchu-shi, Tokyo 183-8561, Japan

M. Kagami · T. Ogata
Division of Clinical Genetics and Molecular Medicine,
National Center for Child Health and Development,
2-10-1 Okura,
Seatagaya-ku, Tokyo 157-8535, Japan

Introduction

Uniparental disomy (UPD) refers to the inheritance of a pair of chromosomes from only one parent. UPD is a relatively common phenomenon. The inheritance of both, or parts of both, maternal chromosomes (heterodisomic maternal UPD) has been found to become more prevalent as parental age becomes more advanced [1]. It is well established that UPD for chromosomes 6, 7, 11, 14 and 15 is associated with recognized syndromes, including Prader-Willi syndrome (maternal UPD 15), Angelman syndrome (paternal UPD 15), and Beckwith-Wiedemann syndrome (paternal UPD 11) [2].

The paternal UPD 14 phenotype (upd(14)pat) is a recently recognized genetic condition that is caused by an aberration of the imprinting center in chromosome 14. The clinical hallmarks of upd(14)pat are thoracic hypoplasia and abdominal wall defect. Mild facial dysmorphism and developmental delay are also noted. In addition, upd(14)pat presents with a distinctive radiological finding: the "coat-hanger" appearance of the ribs and a bell-shaped thorax [3]. In the past, upd(14)pat was often misdiagnosed as bone dysplasias with thoracic hypoplasia, as in Jeune syndrome [4], because attention was not paid to the morphological differences of the thorax between upd(14)pat and other genetic bone diseases. Previous reports on

upd(14)pat have been based on a single case or a limited number of cases. To date, there has been no radiological report involving a large series of upd(14)pat cases. Although a previous report suggested that the dysmorphic thorax in upd(14)pat ameliorated in the mid-childhood period [5], it remains to be determined how the thoracic deformity in upd (14)pat evolves with age. The purpose of this study was to quantitatively determine the differences in the thoracic deformity between upd(14)pat and other genetic bone diseases, and to establish the age-dependent radiological evolution of the thoracic hypoplasia in upd(14)pat.

Materials and methods

The subjects comprised 11 children (6 girls and 5 boys) with upd(14)pat phenotypes proven on molecular grounds [5, 6]. Three of the 11 children had been managed in our hospital, and 8 were referred to our institution for molecular diagnosis. The molecular diagnoses included seven cases of paternal uniparental disomy, two of microdeletion and two of epimutation. The initial radiographs available for the analysis were obtained in the neonatal period (n=8), and at 7, 24 and 32 months of age (n=1). Sequential radiological evaluation was feasible in 4 of 11 children up to 5 years of age. The study was approved by the institutional review board at the National Center for Child Health and Development.

To assess for the "coat-hanger" sign, the angle between the 6th posterior rib and the horizontal axis was measured (coat hanger angle, CHA; an upward angle was defined as +, and a downward angle as −). The ratio of the mid- to widest thorax diameter (M/W ratio) was calculated for the bell-shaped thorax (Figs. 1, 2). For comparison, both indexes were evaluated in nine cases with bone dysplasia with thoracic hypoplasia, including thanatophoric dysplasia (n=6), Ellis-van Creveld syndrome (n=2) and asphyxiating thoracic dysplasia (n=1). These cases were selected from our radiology database. The children's ages ranged from 21 weeks of gestation to 6 years of age (mean: 11 months of age). Both indexes were also evaluated in five children with respiratory distress syndrome (RDS) and without skeletal abnormalities that could be assessed to determine the evolution of the normal thoracic morphology. In the RDS group, serial follow-up radiographs were available from the neonatal period up to 2 years to 6 years of age (mean 4.2). The measurement of CHA and M/W ratio was performed using an accessory digital tool from a PACS

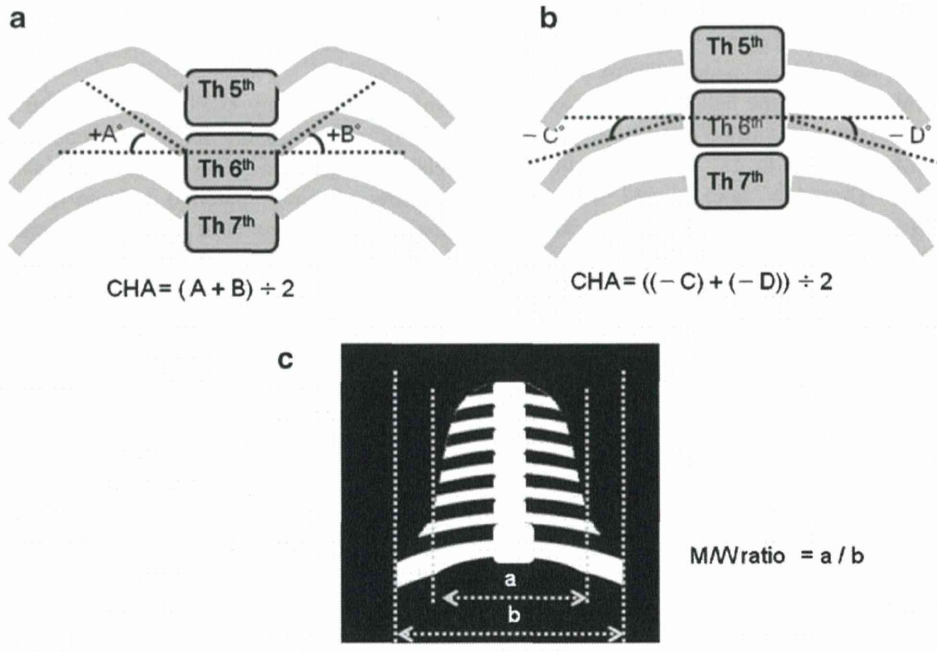

Fig. 1 **a**, **b** Diagram of coat-hanger angle (CHA) and mid/widest ratio. CHA refers to the average of the angles between the peak point of both 6th posterior ribs and the horizontal axis. If there is no peak point of the 6th posterior ribs, the center of the ribs is utilized instead. The horizontal axis is defined as a line passing through two points of both 6th cost-vertebral junctions. An upward angle is defined as +, and a downward angle as −. CHA is thought to be a quantitative index of the coat-hanger sign. **c** The ratio of mid- to widest thorax (M/W ratio) refers to the ratio of the narrowest diameter of the mid-thorax to the widest diameter of the basal thorax. In most cases with upd(14)pat, the thorax showed medial concavity with the top of approximately the 6th rib (the narrowest mid-thorax) and downward sloping toward the 9th to 11th ribs (the widest basal thorax). M/W ratio is thought to be a quantitative index of dysmorphic bell-shaped thorax

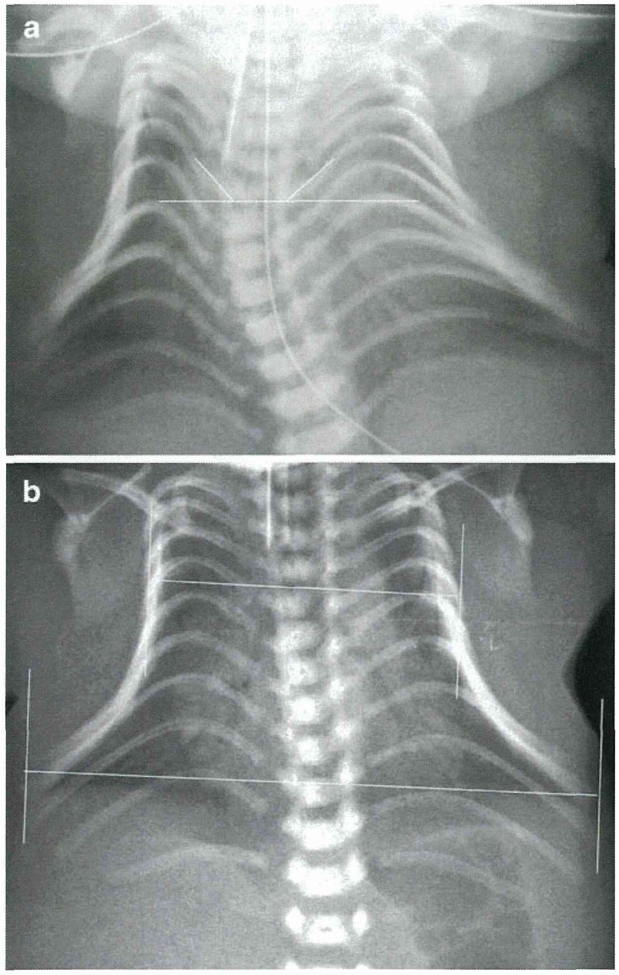

Fig. 2 Examples of CHA and M/W ratio. **a** The 6th posterior ribs show upward bowing that provides the coat-hanger sign. The CHA of this case (patient #7 in Table 1) was 45° (the measurement was 48° for the right and 42° for the left). **b** The M/W ratio was 58% in this case (patient #5 in Table 1). This is an example of severe bell-shaped thorax in upd(14)pat

system (Centricity ™ RA 1000 Ver.3.0, GE Healthcare, Milwaukee, WI) on the PACS monitor, or using area and protractor commercial software (Lenara Ver2.21, Vector, Tokyo) on a personal computer monitor. An unpaired two-tailed t-test was used for statistical evaluation.

Results

Clinical and measurement data are summarized in Table 1 and Fig. 3. All 11 children with upd(14)pat showed a severe upward sweep of the posterior rib or increased CHA, ranging from +28.5 to 45° (mean ± SD; 35.1°±5.2) (Figs. 2, 3). Children with bone dysplasias presented with variable manifestations of the posterior rib, and CHA ranged from −19.8 to 21° (mean ± SD; −3.3±13°) (Figs. 3, 4). The difference in CHA was statistically significant between the upd(14)pat and bone dysplasia groups ($P<0.01$). According to this result, approximately +25° was the estimated cut-off line of CHA to differentiate upd(14)pat from skeletal dysplasias (Fig. 3). The M/W ratio ranged from 58% to 93% (mean±SD; 75.4±10) in the upd(14)pat group, while it ranged between 80% and 92% (mean±SD; 86.8±3.3) in the skeletal dysplasia group (Fig. 3). The difference an unpaired two-tailed t-test in the M/W ratio was, though statistically significant, less conspicuous than that in CHA ($P<0.05$). There was considerable overlap in the range of the M/W ratio between the upd(14)pat and skeletal dysplasia groups.

The age-dependent evolution of CHA and M/W ratio in the upd(14)pat and RDS groups is shown in Fig. 5. In the four children with upd(14)pat, CHA remained unaltered regardless of age, ranging from 25° to 45°. In the RDS group ($n=5$), CHA was constant regardless of age, ranging from −6.4 to 10° (mean −0.6) at birth and from −8 to 7.3° thereafter (Fig. 5). The M/W ratio of the upd(14)pat group was smaller than that of the RDS group in the neonatal period. However, it increased gradually with age and finally caught up with that observed in the RDS group (Figs. 6, 7).

Discussion

The clinical manifestations of upd(14)pat have been well established to date. The hallmarks of this condition include a small thorax, laryngomalacia, hypoplastic abdominal wall, short limbs with joint contractures, craniofacial dysmorphism, and mental retardation [2]. In addition, several reports on the prenatal diagnosis of upd(14)pat suggested the common occurrence of polyhydramnios and preterm delivery in upd(14)pat [2, 7]. A few reports on upd (14)pat have detailed the radiological manifestations, such as disproportionately short limbs, spurring of lower femoral and upper tibial metaphyses, absent glenoid fossa, shortened iliac wing with flaring, thin and elongated clavicle, hypoplastic scapular neck, kyphoscoliosis, hypoplasia of the maxilla and mandible, a broad nasal bridge, wide sutures and multiple wormian skull bones, contractures of the wrists with ulnar deviation, and stippled calcification [3, 8–10]. However, these findings are so mild that alone they do not determine the diagnosis. Instead, the distinctive thoracic deformity in upd(14)pat, termed the coat-hanger sign as introduced by Offiah et al. [3], enables a definitive diagnosis to be made. Sutton et al. [8] described the thoracic deformity of upd(14)pat as "anterior ribs bowed caudally (downward), and posterior portions of the ribs bowed cranially (upward)," and these configurations are combined in the characteristic coat-hanger sign of the ribs

Table 1 Summary of clinical details, measurement of rib angle, coat-hanger angle (CHA), and ratio of mid- to widest thorax (M/W ratio). *GW* gestational week, *TD* thanatophoric dysplasia, *ATD* asphyxiating thoracic dysplasia, *EvC* Ellis-van Creveld syndrome, *RDS* respiratory distress syndrome

Case	Gender	Age (months)[a]	Molecular or clinical diagnosis	Right rib angle (°)	Left rib angle (°)	CHA (°)	M/W ratio (%)
upd(14)pat patients							
1	f	0	upd	36	31	33.5	80
2	m	0	upd	43	41	42	66
3	m	0	upd	27	46	36.5	80
4	m	7	upd	32	38	35	80
5	m	0	deletion	27	30	28.5	58
6	f	0	Epimutation	35	23	29	77
7	f	0	Epimutation	48	42	45	65
8	f (45,XX)	0	upd	30	34	32	69
9	f	0	upd	46	32	39	74
10	m	24	upd	28	38	33	87
11	f	32	decision	32	33	32.5	93
mean		5.7		35	35.82	35.1	75.4
TD group patients							
1	m	21GW	TD	−9.9	−13.7	−11.8	80
2	f	6	TD	−3.7	12	1	85.6
3	m	21GW	TD	−11.7	−13.9	−12.8	86
4	Unknown	20GW	TD	−19.6	−20	−19.8	86
5	m	0	TD	7	−12	−2.5	87
6	m	21GW	TD	−15	−21	−18	87
7	m	84	ATD	4	2	3	88
8	f	11	EvC	9.6	10.3	9.95	90
9	m	24	EvC	14	28	21	92
mean		11		−2.8	−3.1	−3.3	86.8
RDS patients							
1	m	0	RDS	1.8	4	2.9	90
2	m	0	RDS	1.2	−14	−6.4	81.7
3	m	0	RDS	−6.9	−4.1	−5.2	84
4	m	0	RDS	−6	−2	−4	91
5	f	0	RDS	11.3	8.7	10	85
mean		0		0.28	−1.48	−0.54	86.3

[a] Age at which time the initial radiograph was available

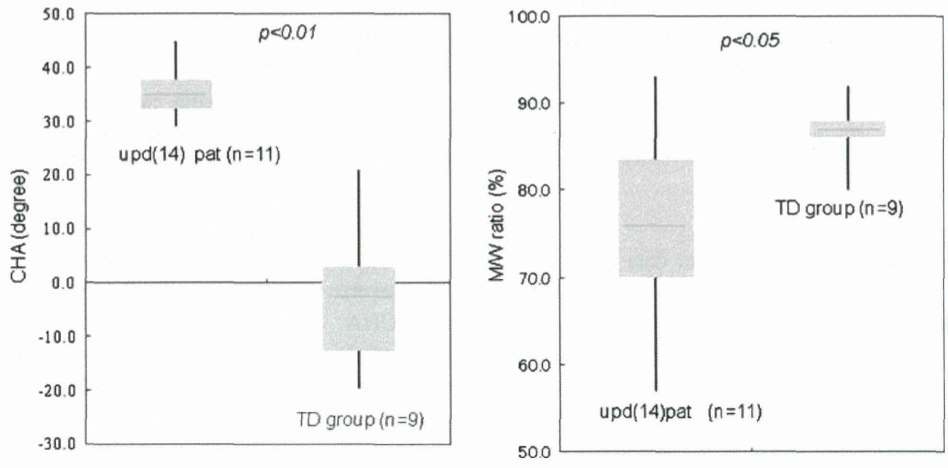

Fig. 3 Box plot of CHA and M/W ratio with the median, interquartile interval and range

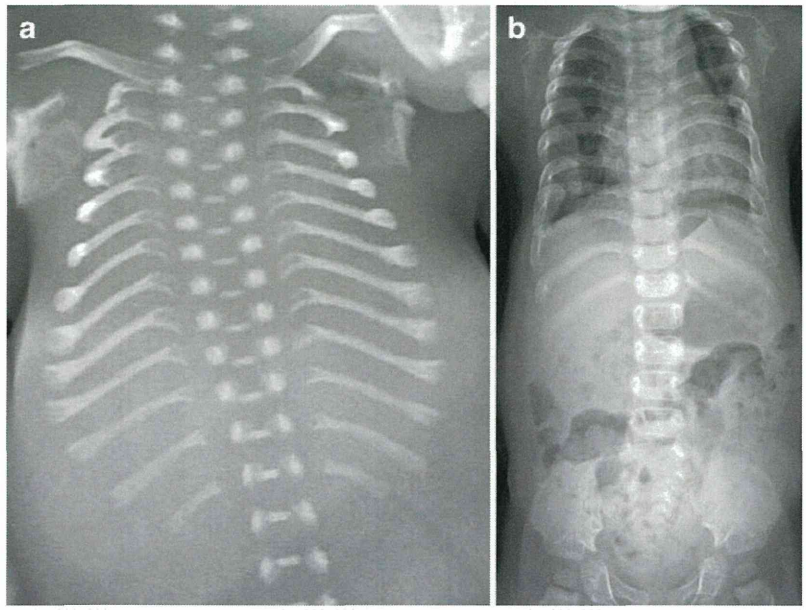

Fig. 4 Examples of the thoracic appearance and measurement of bone dysplasias with thoracic hypoplasia. **a** Thanatophoric dysplasia (TD) type 1 (stillbirth at 21 weeks of gestation). Note a narrow thorax with cupped anterior ends as well as short long bones with metaphyseal cupping. The posterior ribs show downward sloping. The CHA was −18°, and the M/W ratio was 87%. Despite the presence of severe thoracic hypoplasia in TD, its morphology is different from that seen in upd(14)pat (Fig. 2). **b** Ellis-van Creveld (EvC) syndrome (2 years of age). The thorax appears narrow, and a trident appearance of the acetabula is seen. Posterior ribs show upward sloping. The CHA was 21°, and the M/W ratio was 92%. The morphological pattern of the thorax differs from that of upd(14)pat

on the chest radiograph. Sutton et al. concluded that the skeletal phenotype in upd(14)pat involves primarily the axial skeleton, with little to no effect on the long bones. Very small changes of the long bones in upd(14)pat correspond with those of the mouse model (UPD of the distal segment of mouse chromosome 12) [11]. Consequently, it is assumed that imprinted genes on human chromosome 14 and mouse chromosome 12 play a role in axial skeletal formation and ossification [8, 11].

In the subsequent articles on upd(14)pat, all 11 affected children presented unexceptionally with the coat-hanger sign [5, 6, 12]. It was thought that the upward posterior rib bowing and downward anterior rib bowing (the coat-hanger appearance) in upd(14)pat contrast with the horizontally oriented ribs generally seen in disorders with thoracic hypoplasia. Based on the radiological sign, along with other radiological findings, it is not difficult to differentiate upd(14)pat from other genetic disorders involv-

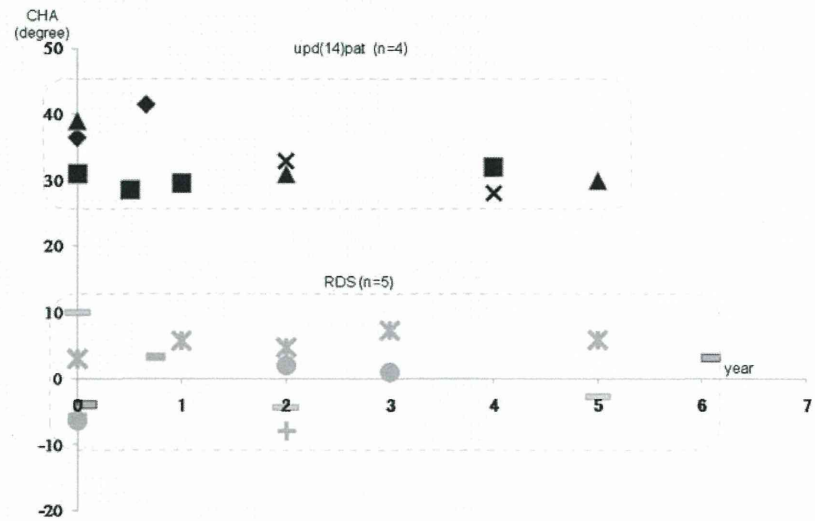

Fig. 5 Comparative observation of age-dependent transition of CHA between the upd(14)pat and respiratory distress syndrome (RDS) groups. Individual shapes represent individual patients

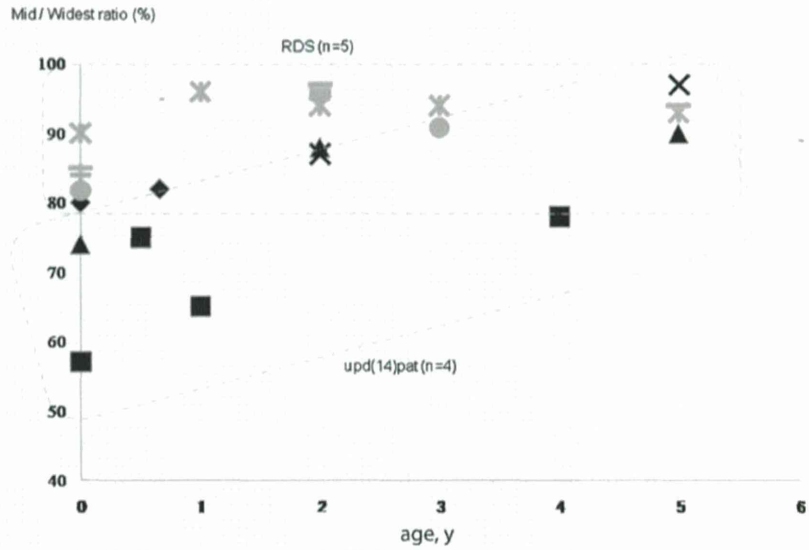

Fig. 6 Comparative observation of age-dependent transition of M/W ratio between the upd(14) pat and RDS groups. Individual shapes represent individual patients

ing thoracic hypoplasia, such as thanatophoric dysplasia, asphyxiating thoracic dysplasia and metatropic dysplasia [13]. However, there are several disorders wherein thoracic hypoplasia is the sole radiological hallmark, including Barnes syndrome, Shwachman-Diamond syndrome and the mildest cases of asphyxiating thoracic hypoplasia. Thus, we thought that quantitative analyses of the coat-hanger sign could elucidate how different the thoracic hypoplasia

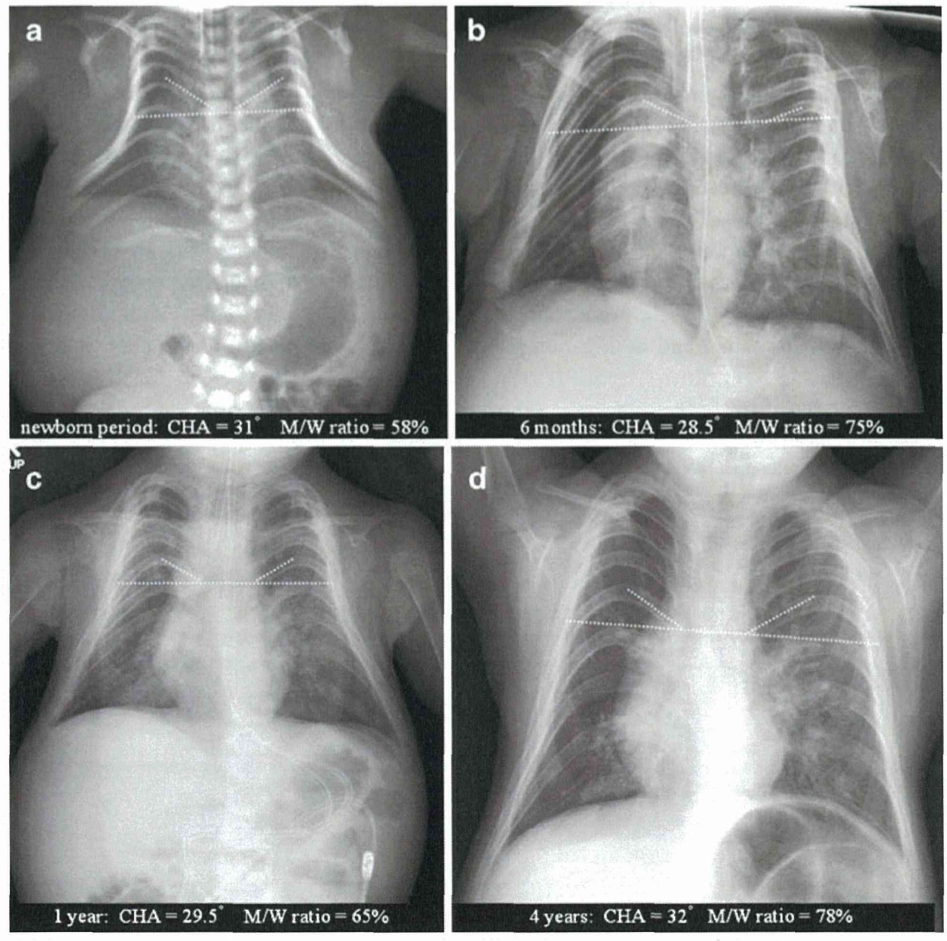

Fig. 7 Serial images of the thorax deformity in upd(14)pat. In this case, four images taken at different ages were available: (**a**) neonatal period, (**b**) 6 months, (**c**) 1 year and (**d**) 4 years. The CHA was almost consistent regardless of age, while the M/W ratio increased with advancing age. The coat-hanger sign and bell-shaped thorax are readily identifiable in the neonatal period. The diagnosis is not straightforward in childhood, yet close observation combined with CHA measurement points to the coat-hanger sign

in upd(14)pat is from the thoracic hypoplasia in other genetic disorders, and presumed that the measurement of CHA (mean 35.1°) and M/W ratio (mean 75.4%) might be helpful when the diagnosis of upd(14)pat is in question. As comparison groups, we included not only cases of severe bone dysplasias but also RDS. Neonates with RDS may present with a small chest [14], and it is not uncommon for them to undergo repeated examinations of chest radiographs because of the association with chronic lung disease.

Kagami et al. [5] reported the age-dependent evolution of the thoracic deformity of upd(14)pat in two children, which was said to ameliorate in mid-childhood. Their observation corresponded with the improvement of the M/W ratio with age described here. By contrast, however, CHA persisted consistently until mid-childhood. This finding indicates that the coat-hanger sign is still discernable during mid-childhood. Radiological findings are presumed to be the only clue to the presence of upd(14)pat after mid-childhood. Serial radiographs (newborn, 2 years and 9 years), as illustrated by Cotter et al. [15] also warrant our observation.

A drawback of this study is that it includes a limited number of cases and available radiographs with uneven quality, such as chest radiographs with some obliquity and radiographs taken in the supine position in the neonatal period vs. the upright position in childhood. Even taking into account these technical problems, however, we believe that our quantitative analyses, particularly the measurement of the CHA, are a valid way to characterize the distinctive thoracic deformity in upd(14)pat.

Conclusion

The coat-hanger sign of upd(14)pat was quantitatively represented by CHA, and was found to be more severe than that seen in other genetic bone diseases and to persist into early childhood; thus, the findings will help in the diagnosis of upd(14)pat even after infancy. By contrast, the bell-shaped thorax represented by M/W ratio was significant only in the neonatal period, and its diagnostic value declined with age.

References

1. Kotzot D (2004) Advanced parental age in maternal uniparental disomy (UPD): implication for the mechanism of formation. Eur J Hum Genet 12:343–346
2. Towner D, Yang SP, Shaffer G (2001) Prenatal ultrasound findings in a fetus with paternal uniparental disomy 14q12-qter. Ultrasound Obstet Gynecol 18:268–271
3. Offiah AC, Cornette L, Hall CM (2003) Paternal uniparental disomy 14: introducing the "coat-hanger" sign. Pediatr Radiol 33:509–512
4. Stevenson DA, Brothman AR, Chen Z et al (2004) Paternal uniparental disomy of chromosome 14: confirmation of a clinically-recognizable phenotype. Am J Med Genet A 130A:88–91
5. Kagami M, Nishimura G, Okuyama T et al (2005) Segmental and full paternal isodisomy for chromosome 14 in three patients: narrowing the critical region and implication for the clinical feature. Am J Med Genet A 138A:127–132
6. Kurosawa K, Sasaki H, Yamanaka M et al (2002) Paternal UPD 14 is responsible for a distinctive malformation complex. Am J Med Genet 110:268–272
7. Yamanaka M, Ishikawa H, Saito K et al (2010) Prenatal findings of paternal uniparental disomy 14: report of four patients. Am J Med Genet 152A:789–791
8. Sutton VR, McAlister WH, Bertin TK et al (2003) Skeletal defect in paternal uniparental disomy for chromosome 14 are re-capitulated in the mouse model (paternal uniparental disomy 12). Hum Genet 113:447–451
9. Mattes J, Whitehead B, Liehr T et al (2007) Paternal uniparental isodisomy for chromosome 14 with mosaicism for a supernumerary marker chromosome 14. Am J Med Genet 143A:2165–2171
10. Irving MD, Bulting K, Kanber D et al (2010) Segmental paternal uniparental disomy (patUPD) of 14q32 with abnormal methylation elicites the characteristic features of complete pat UPD14. Am J Med Genet 152A:1942–1950
11. Georgiades P, Watkins M, Surani MA et al (2000) Parental origin-specific developmental defects in mice with uniparental disomy for chromosome 12. Development 127:4719–4728
12. Kagami M, Sekita Y, Nishimura G et al (2008) Deletions and epimutations affecting the human 14q32.2 imprinted region in individuals with paternal and maternal upd(14)-like phenotypes. Nat Genet 40:237–242
13. Spranger JW (2002) Asphyxiating thoracic dysplasia. In: Spranger JW, Brill PW, Poznanski A (eds) Bone dysplasia, an atlas of genetic disorders of skeletal development, 2nd edn. Oxford University Press, New York, pp 125–129
14. Swischuk LW (2004) Chapter 1. Respiratory system; respiratory distress in the newborn. In: Swischuk LE (ed) Imaging of the newborn, infant, and young child, 5th edn. Lippincott, Williams & Wilkins, Philadelphia, pp 29–36
15. Cotter PD, Kaffe S, McCurdy LD et al (1997) Paternal uniparental disomy for chromosome 14: a case report and review. Am J Med Genet 70:74–79

Short report

Parthenogenetic chimaerism/mosaicism with a Silver-Russell syndrome-like phenotype

K Yamazawa,[1,2] K Nakabayashi,[3] M Kagami,[1] T Sato,[1] S Saitoh,[4] R Horikawa,[5] N Hizuka,[6] T Ogata[1]

► Additional figures, tables and an appendix are published online only. To view these files, please visit the journal online (http://jmg.bmj.com).

[1]Departments of Endocrinology and Metabolism, National Research Institute for Child Health and Development, Tokyo, Japan
[2]Department of Physiology, Development & Neuroscience, University of Cambridge, Cambridge, UK
[3]Maternal-Fetal Biology, National Research Institute for Child Health and Development, Tokyo, Japan
[4]Department of Pediatrics, Hokkaido University Graduate School of Medicine, Sapporo, Japan
[5]Division of Endocrinology and Metabolism, National Children's Hospital, Tokyo, Japan
[6]Department of Medicine, Institute of Clinical Endocrinology, Tokyo Women's Medical University, Tokyo, Japan

Correspondence to
Dr Tsutomu Ogata, Department of Endocrinology and Metabolism, National Research Institute for Child Health and Development, 2-10-1 Ohkura, Setagaya, Tokyo 157-8535, Japan; tomogata@nch.go.jp

Received 20 March 2010
Revised 6 May 2010
Accepted 8 May 2010
Published Online First 3 August 2010

ABSTRACT

Introduction We report a 34-year-old Japanese female with a Silver-Russell syndrome (SRS)-like phenotype and a mosaic Turner syndrome karyotype (45,X/46,XX).

Methods/Results Molecular studies including methylation analysis of 17 differentially methylated regions (DMRs) on the autosomes and the *XIST*-DMR on the X chromosome and genome-wide microsatellite analysis for 96 autosomal loci and 30 X chromosomal loci revealed that the 46,XX cell lineage was accompanied by maternal uniparental isodisomy for all chromosomes (upid(AC)mat), whereas the 45,X cell lineage was associated with biparentally derived autosomes and a maternally derived X chromosome. The frequency of the 46,XX upid(AC)mat cells was calculated as 84% in leukocytes, 56% in salivary cells, and 18% in buccal epithelial cells.

Discussion The results imply that a parthenogenetic activation took place around the time of fertilisation of a sperm missing a sex chromosome, resulting in the generation of the upid(AC)mat 46,XX cell lineage by endoreplication of one blastomere containing a female pronucleus and the 45,X cell lineage by union of male and female pronuclei. It is likely that the extent of overall (epi)genetic aberrations exceeded the threshold level for the development of SRS phenotype, but not for the occurrence of other imprinting disorders or recessive Mendelian disorders.

Although a mammal with maternal uniparental disomy for all chromosomes (upd(AC)mat) is incompatible with life because of genomic imprinting,[1] a mammal with a upd(AC)mat cell lineage could be viable in the presence of a co-existing normal cell lineage. In the human, Strain *et al*[2] have reported 46,XX peripheral blood cells with maternal uniparental isodisomy for all chromosomes (upid(AC)mat) in a 1.2-year-old phenotypically male patient with aggressive behaviour, hemifacial hypoplasia and normal birth weight. Because of the 46,XX disorders of sex development, detailed molecular studies were performed, revealing the presence of a normal 46,XY cell lineage in a vast majority of skin fibroblasts and a upid(AC)mat 46,XX cell lineage in nearly all blood cells. In addition, although the data are insufficient to draw a definitive conclusion, Horike *et al*[3] have also identified 46,XX peripheral blood cells with possible upd(AC)mat in a phenotypically male patient through methylation analyses for plural differentially methylated regions (DMRs) in 11 patients with Silver–Russell syndrome (SRS)-like phenotype. This patient was found to have a normal 46,XY cell lineage and a triploid 69,XXY cell lineage in skin fibroblasts.

However, such patients with a upd(AC)mat cell lineage remain extremely rare, and there is no report describing a human with such a cell lineage in the absence of a normal cell lineage. Here, we report a female patient with a upid(AC)mat 46,XX cell lineage and a non-upd 45,X cell lineage who was identified through genetic screenings of 103 patients with SRS-like phenotype.

MATERIALS AND METHODS

Case report

This Japanese female patient was conceived naturally and born at 40 weeks of gestation by a normal vaginal delivery. At birth, her length was 44.0 cm (−3.1 SD), her weight 2.1 kg (−2.9 SD) and her occipitofrontal head circumference (OFC) 30.5 cm (−2.3 SD). The parents and the younger brother were clinically normal (the father died from a traffic accident).

At 2 years of age, she was referred to us because of growth failure. Her height was 77.7 cm (−2.5 SD), her weight 8.45 kg (−2.6 SD) and her OFC 43.5 cm (−2.5 SD). Physical examination revealed several SRS-like somatic features such as triangular face, right hemihypoplasia and bilateral fifth finger clinodactyly. She also had developmental retardation, with a developmental quotient of 56. Endocrine studies for short stature were normal as were radiological studies. Cytogenetic analysis using lymphocytes indicated a low-grade mosaic Turner syndrome (TS) karyotype, 45,X[3]/46,XX[47]. Thus, a screening of TS phenotype[4] was performed, detecting horseshoe kidney but no body surface features or cardiovascular lesion. Chromosome analysis was repeated at 6 and 32 years of age using lymphocytes, revealing a 45,X[8]/46,XX[92] karyotype and a 45,X[12]/46,XX[88] karyotype, respectively. On the last examination at 34 years of age, her height was 125.0 cm (−6.2 SD), her weight 37.5 kg (−2.0 SD) and her OFC 51.2 cm (−2.8 SD). She was engaged in a simple work and was able to get on her daily life for herself.

Sample preparation

This study was approved by the Institutional Review Board Committees at National Center for Child health and Development. After obtaining written informed consent, genomic DNA was extracted from leukocytes of the patient, the mother and the brother and from salivary cells, which comprise ~40% of buccal epithelial cells and ~60% of leukocytes,[5] of the patient. Lymphocyte metaphase spreads and leukocyte RNA were also

obtained from the patient. Leukocytes of healthy adults and patients with imprinting disorders were utilised for controls.

Primers and probes

The primers utilised in this study are summarised in supplementary methods and supplementary tables 1–3.

DMR analyses

We first performed bio-combined bisulfite restriction analysis (COBRA)[6] and bisulfite sequencing of the *H19*-DMR (A) on chromosome 11p15.5 by the previously described methods[7] and methylation-sensitive PCR analysis of the *MEST*-DMR (A) on chromosome 7q32.2 by the previously described methods[8] with minor modifications (the methylated and unmethylated allele-specific primers were designed to yield PCR products of different sizes, and the PCR products were visualised on the 2100 Bioanalyzer (Agilent, Santa Clara, California, USA)). This was because hypomethylation (epimutation) of the normally methylated *H19*-DMR of paternal origin and maternal uniparental disomy 7 are known to account for 35–65% and 5–10% of SRS patients, respectively.[9 10] In addition, fluorescence in situ hybridisation (FISH) analysis was performed with a ~84-kb RP5-998N23 probe containing the *H19*-DMR (BACPAC Resources Center, Oakland, California, USA). We also examined multiple other DMRs by bio-COBRA. The ratio of methylated clones (the methylation index) was calculated using peak heights of digested and undigested fragments on the 2100 Bioanalyzer using 2100 expert software.

Genome-wide microsatellite analysis

Microsatellite analysis was performed for 96 autosomal loci and 30 X chromosomal loci. The segment encompassing each locus was PCR-amplified, and the PCR product size was determined on the ABI PRISM 310 autosequencer using GeneScan software (Applied Biosystems, Foster City, California, USA).

PCR analysis for Y chromosomal loci

Standard PCR was performed for six Y chromosomal loci. The PCR products were electrophoresed using the 2100 Bioanalyzer.

Expression analysis

Quantitative real-time reverse transcriptase PCR analysis was performed for three paternally expressed genes (*IGF2*, *SNRPN* and *ZAC1*) and four maternally expressed genes (*H19*, *MEG3*, *PHLDA2* and *CDKN1C*) that are known to be variably (usually weakly) expressed in leukocytes (UniGene, http://www.ncbi.nlm.nih.gov/sites/entrez?db=unigene), using an ABI Prism 7000 Sequence Detection System (Applied Biosystems). *TBP* and *GAPDH* were utilised as internal controls.

RESULTS

DMR analyses

In leukocytes, the bio-COBRA indicated severely hypomethylated *H19*-DMR, and bisulfite sequencing combined with *rs2251375* SNP typing for 30 clones revealed maternal origin of 29 hypomethylated clones and non-maternal (paternal) origin of a single methylated clone in this patient (figure 1A). Thus, the marked hypomethylation of the *H19*-DMR was caused by predominance of maternally derived clones rather than hypomethylation of the *H19*-DMR of paternal origin. FISH analysis for 100 lymphocyte metaphase spreads excluded an apparent deletion of the paternally derived *H19*-DMR or duplication of the maternally derived *H19*-DMR (Supplementary figure 1). Methylation-sensitive PCR amplification for the *MEST*-DMR delineated a major peak for the methylated allele and a minor peak for the unmethylated allele (figure 1B). This also indicated the predominance of maternally derived clones and the co-existence of a minor portion of paternally derived clones. Furthermore, autosomal DMRs invariably exhibited markedly abnormal methylation patterns consistent with predominance of maternally inherited DMRs, whereas the methylation index of the *XIST*-DMR on the X chromosome remained within the female reference range (figure 1C). The abnormal methylation patterns were less obvious in salivary cells (thus, in buccal epithelial cells) than in leukocytes, except for the methylation index for the *XIST*-DMR that mildly exceeded the female reference range (figure 1A–C).

Microsatellite analysis

Major peaks consistent with maternal uniparental isodisomy and minor peaks of non-maternal (paternal) origin were identified for at least one locus on each autosome, with the minor peaks of non-maternal origin being more obvious in salivary cells than in leukocytes (figure 1D and supplementary table 4). Furthermore, the frequency of the upid(AC)mat cells was calculated as 84% in leukocytes, 56% in salivary cells and 18% in epithelial buccal cells, using the area under curves for the maternally and the non-maternally inherited peaks (supplementary note). Such minor peaks of non-maternal origin were not detected for all the 30 X chromosomal loci examined.

PCR analysis for Y chromosomal loci

PCR amplification failed to detect any trace of Y chromosome-specific bands in leukocytes and salivary cells (Supplementary figure 2).

Expression analysis

Expression analysis using control leukocytes indicated that, of the seven examined genes, *SNRPN* expression alone was strong enough to allow for a precise assessment (Supplementary figure 3). *SNRPN* expression was extremely low in this patient (figure 1E).

DISCUSSION

These results imply that this patient had a upid(AC)mat 46,XX cell lineage and a non-upd 45,X cell lineage. Indeed, methylation patterns of the *XIST*-DMR is explained by assuming that the two X chromosomes in the upid(AC)mat cells undergo random X-inactivation and that 45,X cells with the methylated *XIST*-DMR on a single active X chromosome[11] are relatively prevalent in buccal epithelial cells. Furthermore, lack of non-maternally derived minor peaks for microsatellite loci on the X chromosome is explained by assuming that the two X chromosomes in the upid(AC)mat cells and the single X chromosome in the 45,X cells are derived from a common X chromosome of maternal origin, with no paternally derived sex chromosome. It is likely, therefore, that a parthenogenetic activation took place around the time of fertilisation of a sperm missing a sex chromosome, resulting in the generation of the 46,XX cell lineage with upid (AC)mat by endoreplication (the replication of DNA without the subsequent completion of mitosis) of one blastomere containing a female pronucleus and the 45,X cell lineage with biparentally derived autosomes and a maternally derived X chromosome by union of male and female pronuclei (figure 2), although it is also possible that a paternally derived sex chromosome was present in the sperm but was lost from the normal

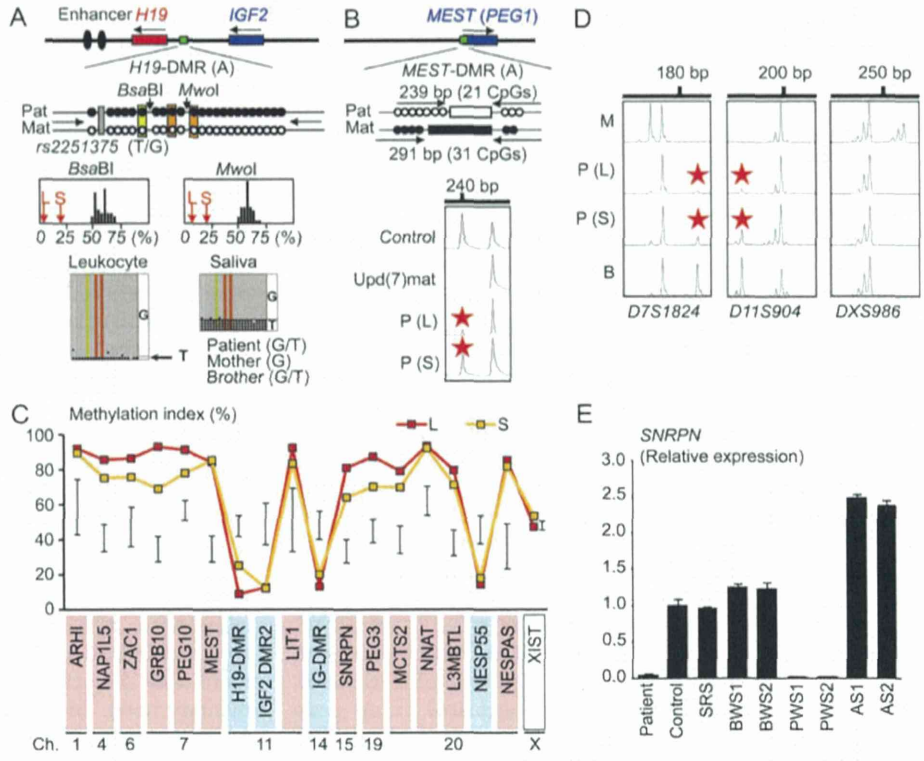

Figure 1 Representative molecular results. Pat, paternally derived allele; Mat, maternally derived allele; P, patient; M, mother; B, brother; L, leukocytes; and S, salivary cells. Filled and open circles in A and B represent methylated and unmethylated cytosine residues at the CpG dinucleotides, respectively. A. Methylation patterns of the *H19*-DMR (A) harbouring 23 CpG dinucleotides and the T/G SNP (*rs2251375*) (a grey box). The PCR products are digested with *Bsa*BI when the cytosine at the sixth CpG dinucleotide (highlighted in yellow) is methylated and with *Mwo*I when the two cytosines at the ninth and the 11th CpG dinucleotides (highlighted in orange) are methylated. For the bio-COBRA data, the black histograms represent the distribution of methylation indices (%) in 50 control participants, and L and S denote the methylation indices for leukocytes and salivary cells of this patient, respectively. For the bisulfite sequencing data, each line indicates a single clone. B. Methylated and unmethylated allele-specific PCR analysis for the *MEST*-DMR (A). In a control participant, the PCR products for methylated and unmethylated alleles are delineated, and the unequal amplification is consistent with a short product being more easily amplified than a long product. In a previously reported patient with upd(7)mat,[8] the methylated allele only is amplified. In this patient, major peaks for the methylated allele and minor peaks for the unmethylated allele (red asterisks) are detected. C. Methylation patterns for the 18 DMRs examined. The DMRs highlighted in blue and pink are methylated after paternal and maternal transmissions, respectively. The black vertical bars indicate the reference data (maximum–minimum) in 20 normal control participants, using leukocyte genomic DNA (for the *XIST*-DMR, 16 female data are shown). D. Representative microsatellite analysis. Minor peaks (red asterisks) have been identified for *D7S1824* and *D11S904* but not for *DXS986* of the patient. Since the peaks for *D7S1824* and *D11S904* are absent in the mother and clearly present in the brother, they are assessed to be of paternal origin. E. Relative expression level (mean ± SD) of *SNRPN* on chromosome 15. The data have been normalised against *TBP*. SRS, an SRS patient with an epimutation (hypomethylation) of the *H19*-DMR; BWS1, a BWS patient with an epimutation (hypermethylation) of the *H19*-DMR; BWS2, a BWS patient with upd(11)pat; PWS1, a PWS patient with upd(15)mat; PWS2, a PWS patient with an epimutation (hypermethylation) of the *SNRPN*-DMR; AS1, an Angelman syndrome (AS) patient with upd(15)pat; and AS2, an AS patient with an epimutation (hypomethylation) of the *SNRPN*-DMR.

cell lineage at the very early developmental stage. Hence, in a strict sense, this patient is neither a chimera resulting from the fusion of two different zygotes nor a mosaic caused by a mitotic error of a single zygote. In this regard, a triploid cell stage is assumed in the generation of a upid(AC)mat cell lineage, and such triploid cells may have been detected in skin fibroblasts of the patient reported by Horike *et al*.[3]

The upid(AC)mat cells accounted for the majority of leukocytes even in adulthood of this patient, despite global negative selective pressure.[12 13] This phenomenon, though intriguing, would not be unexpected in human studies because leukocytes are usually utilised for genetic analyses. Rather, if the upid(AC)mat cells were barely present in leukocytes, they would not have been detected. It is likely, therefore, that upid(AC)mat cells have occupied a relatively large portion of the definitive haematopoietic tissues primarily as a stochastic event. Furthermore, parthenogenetic chimera mouse studies have revealed that parthenogenetic cells are found at a relatively high frequency in some tissues/organs including blood and are barely identified in other tissues/organs such as skeletal muscle and liver.[13] Such a possible tissue-specific selection in favour of the preservation of parthenogenetic cells in the definitive haematopoietic tissues may also be relevant to the predominance of the upid(AC)mat cells in leukocytes. In addition, a reduced growth potential of 45,X cells[14] may also have contributed to the skewed ratio of the two cell lineages.

Clinical features of this patient would be determined by several factors. They include: (1) the ratio of two cell lineages in various tissues/organs, (2) the number of imprinted regions or DMRs relevant to the development of specific imprinting disorders (eg, plural regions/DMRs on chromosomes 7 and 11 for SRS[9 10] and a single region/DMR on chromosome 15 for Prader–Willi syndrome (PWS)),[15] (3) the degree of clinical effects of dysregulated imprinted regions/DMRs (an (epi)dominant effect has been

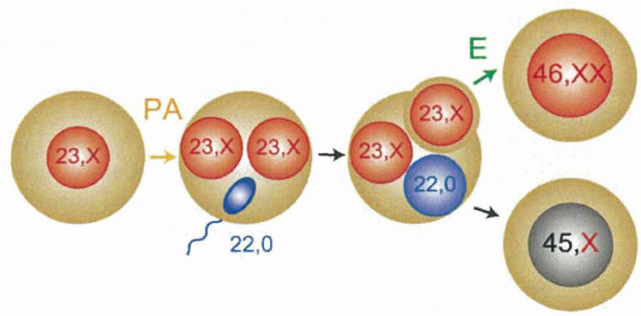

Figure 2 Schematic representation of the generation of the upid(AC)mat 46,XX cell lineage and the non-upd 45,X cell lineage. Polar bodies are not shown. PA, parthenogenetic activation; and E, endoreplication of one blastomere containing a female pronucleus.